WIRELESS COMMUNICATIONS AND MOBILE COMPUTING
Wirel. Commun. Mob. Comput. 2016; **16**:2194–2211
Published online 3 June 2016 in Wiley Online Library (wileyonlinelibrary.com). DOI: 10.1002/wcm.2676

RESEARCH ARTICLE

An underwater acoustic communication scheme exploiting biological sounds†

Ahmad ElMoslimany[1*], Meng Zhou[1], Tolga M. Duman[2] and Antonia Papandreou-Suppappola[1]

[1] School of Electrical,Computer and Energy Engineering (ECEE), Ira A. Fulton Schools of Engineering, Arizona State University, P. O. Box 875706, Tempe, AZ 85287-5706, U.S.A.
[2] Department of Electrical and Electronics Engineering, Bilkent University, Bilkent, Ankara 06800, Turkey

ABSTRACT

Underwater acoustic (UWA) communications have attracted a lot of interest in recent years motivated by a wide range of applications including offshore oil field exploration and monitoring, oceanographic data collection, environmental monitoring, disaster prevention, and port security. Different signaling solutions have been developed to date including non-coherent communications, phase coherent systems, multi-input and multi-output solutions, time-reversal-based communication systems, and multi-carrier transmission approaches. This paper deviates from the traditional approaches to UWA communications and develops a scheme that exploits biomimetic signals. In the proposed scheme, a transmitter maps the information bits to the parameters of a biomimetic signal, which is transmitted over the channel. The receiver estimates the parameters of the received signal and demaps them back to bits to estimate the message. As exemplary biomimetic signals, analytical signal models with nonlinear instantaneous frequency are developed that match mammal sound signatures in the time-frequency plane are developed. Suitable receiver structures as well as performance analysis are provided for the proposed transmission scheme, and some results using data recorded during the Kauai Acomms MURI 2011 UWA communications experiment are presented. Copyright © 2016 John Wiley & Sons, Ltd.

KEYWORDS
biological sounds; underwater acoustic communications; LPI and LPD communication scheme

***Correspondence**
Ahmad ElMoslimany, School of Electrical, Computer and Energy Engineering (ECEE), Ira A. Fulton Schools of Engineering, Arizona State University, P. O. Box 875706, Tempe, AZ 85287-5706, U.S.A.
E-mail: aelmosli@asu.edu

1. INTRODUCTION

Underwater acoustic (UWA) communications are considered as one of the most challenging communication systems in use today. This is because the communication medium is highly time-varying and causes large distortions due to extensive multipath spreads, frequency-dependent path loss, and time selectivity [1]. In addition to the average path loss due to spreading and absorption losses, the received power fluctuates as a result of small-scale fading effects due to multipath propagation. UWA channels are often characterized by significant frequency and time selectivity, because of variations in the underwater environment (e.g., surface waves) or because of the relative motion between the transmitter and the receiver. Furthermore, because the speed of the sound in water is low, the transmitted signal may also undergo time-scaling (severe Doppler) effects, because the carrier frequencies are in the order of the transmit signal bandwidths used.

In this paper, we propose a communication scheme that uses biomimetic signals to transmit digital information. We develop analytical models for certain biomimetic signals, and we parametrize them. Digital data are transmitted by mapping vectors of information bits to a carefully designed set of parameters with values obtained from the biomimetic signal models. To complete the overall system design, we develop appropriate receivers taking into account the specific UWA channel models. The basic premise is the following: because there is no artificial embedding of digital data on a (biological) host signal, the transmitted signal will mimic a natural sound. Such a scenario may have applications in covert communications with low

†Part of this work was presented in the 2013 MTS/IEEE OCEANS in San Diego.

Copyright © 2016 John Wiley & Sons, Ltd.

probability of detection (LPD) and low probability intercept (LPI) characteristics.

There has been significant progress over the years in UWA communications. In earlier UWA communications systems, the main focus was on non-coherent and differentially coherent communication techniques. A breakthrough was the work performed by Stojanovic *et al.* [2], which demonstrated for the first time the feasibility of phase coherent communications via a decision feedback equalizer (DFE). DFE coefficients were updated along with the carrier phase by minimizing the mean squared error in an adaptive fashion. More recently, multi-carrier UWA communication schemes based on orthogonal frequency division multiplexing (OFDM) have also been developed [3]. For UWA communications, OFDM trades off intersymbol interference with intercarrier interference because of the highly time-varying nature of the communication medium, see [4,5] and the references therein. In the last decade, space-time coding techniques (for multi-input multi-output systems) have also been demonstrated successfully for UWA channels [6–9]. Another fundamental line of research in UWA communications was devoted to the time reversal (TR) techniques [10–13], which provide temporal and spatial focus (compression). The temporal focus (shortening of the channel delay spread) mitigates the channel dispersion, while spatial focus mitigates the effects of the channel fading and provides a high signal-to-noise ratio (SNR) at the receiver.

As mentioned previously, a possible application for the proposed biomimetic communication scheme of this work is for covert UWA communications in which we are interested in LPD and/or LPI. That is, we may be interested in transmitting our signals in such a way that the presence of communication cannot be sensed by eavesdroppers (LPD) and/or cannot be demodulated (LPI) except for intended users. Most existing techniques developed for covert communications rely on spread spectrum ideas. For instance, with the direct sequence spread spectrum (DSSS) technique, the transmitted signal is spread, using a spreading code, over a certain frequency band such that its power spectral density goes below the noise level, which makes it difficult to be detected. At the intended receiver, the spreading code is known, hence the signal is despread and the original transmitted signal is retrieved. The key point in using the DSSS is that as long as the spreading code is long enough, an acceptable performance can be achieved. Different communication schemes was developed for UWA covert communications based on spread spectrum techniques [14,15].

A different approach to provide covertness is based on the use of natural sounds in transmission. The bottlenose dolphin sound signals are used for convert communication. Specifically, dolphin whistles are modeled as weighted superpositions of harmonically related sinusoids, and single sinusoidal frequencies are estimated over windowed data [16]. Because of the methodology adopted, the generated signal may sound man-made, which may present a problem in using this approach for LPD/LPI communications under water. There are two other very recent schemes [17,18] that use biological sounds for covert communications are presented. In the first scheme, the authors use dolphin whistles for synchronization purposes and the time interval between dolphin clicks to convey digital information. In the second one, DSSS signals that carry digital data are masked with a relatively loud whale sound.

Coming back to our proposal of using natural sounds for signal transmission where digital data are modulated on the parameters of carefully modeled biological signals, our approach provides a way for which signals generated do not sound artificial because of the way in which they are constructed. In other words, signals matched to mammal sounds could be useful for UWA communications even at relatively high transmit power levels. They can also coexist with other acoustic communication systems without adversely affecting their performance or without being affected by them. Our proposal, as in the two very recent papers [17,18], aims to incorporate biological sounds in UWA communications systems; however, the specific approach used is completely different. A preliminary and brief version of our proposal has already appeared in the literature [19].

The paper is organized as follows. In Section 2, we develop analytical models for the biomimetic signals, and we provide a parametrization for these models. In Section 3, we describe our communication scheme; the signaling scheme and the receiver structure for additive white Gaussian noise (AWGN) channels and multipath channels, respectively. In Section 4, we provide a brief performance analysis and derive bounds on error rates. In Section 5, we present a detailed set of experimental results demonstrating the feasibility of the proposed communication scheme using data recorded in the Kauai Acomms MURI 2011 experiment.

2. BIOMIMETIC SIGNAL MODELING

Cetacean mammals, such as dolphins and whales, have a complicated communication system. Their sound emissions are mainly classified into clicks and whistles [20,21]. Clicks are sonar echolocation signals consisting of short duration, broadband, transient-like pulses that are used to detect, localize, and discriminate objects. Whistles are communication signals that consist of long duration, frequency-modulated, continuous sounds varying in bandwidth, duration, and time-frequency structure. The time-frequency structure of bottlenose dolphin whistles, for example, was determined to have nonlinear frequency modulation (FM) and range in frequency from 200 Hz to 24 kHz. Studies have shown that dolphins in isolation have their own unique characteristic signature whistle and also that they can mimic each other's sounds when placed in groups [22].

The time-frequency variations of dolphin and whale whistles are inspiring for use as biological models in designing transmit waveforms for underwater communications. The UWA communications channel has been

shown to cause nonlinear time-varying changes to the instantaneous frequency of a waveform when transmitted at low frequencies [23]. A communications performance improvement is therefore expected if the time-frequency signature of the transmit waveform is designed to match this nonlinear time-varying change caused by the UWA channel. In [24], dolphin and whale whistle sounds were analyzed using quadratic time-frequency representations (TFRs). Based on this analysis, the time-frequency structure of whistle sounds was modeled to match the instantaneous frequency of generalized frequency-modulated signals. We thus want to use these biomimetic signal models for underwater communication, varying their parameters and nonlinear instantaneous frequency characteristics to match those of real whistle sounds.

2.1. Nonlinear frequency-modulated signals

We define nonlinear frequency-modulated (NFM) signals as [25,26]

$$s(t;\mathbf{b}) = A\,\alpha(t)\,e^{j2\pi(c\,\xi(t/t_r)+f_0 t)}, \tag{1}$$

where $\xi(t/t_r)$ is the signal's phase function, f_0 is the carrier frequency, A is the amplitude, $c \in \mathbb{R}$ is the FM rate, and $t_r > 0$ is a fixed time constant used for unit normalization. The parameter vector $\mathbf{b}$ of the NFM signal in (1) consists of the FM rate c, amplitude A, phase function $\xi(t/t_r)$, and signal duration T_d. We select $\alpha(t) = \sqrt{|\nu(t)|}$, where $\nu(t)$ is the signal's instantaneous frequency (or derivative of the phase function), to ensure that the NFM in (1) is an orthogonal signal. Specifically, using $\nu(t) = \frac{d}{dt}\xi(t/t_r)$, the inner product between two NFM signals with the same amplitude and phase function but different FM rates can be shown to be

$$\begin{aligned}\int_{t\in\mathcal{R}_\xi} & A\sqrt{|\nu(t)|}\,e^{j2\pi(c_1\xi(t/t_r)+f_0 t)} \\ & A\sqrt{|\nu(t)|}\,e^{-j2\pi(c_2\xi(t/t_r)-f_0 t)}\,dt \\ & \overset{(a)}{=} A^2\int_{-\infty}^{\infty} e^{j2\pi c_1 t'}\,e^{-j2\pi c_2 t'}\,dt' \\ & = A^2\,\delta(c_1-c_2),\end{aligned} \tag{2}$$

where (a) follows by change of variables, $\delta(\cdot)$ is the Dirac delta function, and the domain and range of $\xi(t/t_r)$ are assumed to be $\mathcal{R}_\xi$ and $\mathbb{R}$, respectively. Discretizing the real part of the NFM signal using sampling period T_s and $M = \lfloor T_d/T_s \rfloor$ yields

$$\begin{aligned}&s[n;\mathbf{b}] = s(nT_s;\mathbf{b}) = A\sqrt{|\nu[n]|}\cos(2\pi c\,\xi[n] + 2\pi f_0 T_s n)\,, \\ &n = 0,1,\ldots,M-1.\end{aligned} \tag{3}$$

2.2. Biomimetic signal matching

By varying the phase function $\xi(t/t_r)$ in (1), we can obtain different instantaneous frequencies $\nu(t)$ to match the time-frequency structures of cetacean mammal whistles. Specifically, if the TFR of a whistle has a characteristic of a monotonically changing signature, we need to find an NFM whose instantaneous frequency $\nu(t)$ best matches this signature. Table I provides some examples of NFM signals from (1) with $t_r = 1$, together with their phase function $\xi(t/t_r)$ and corresponding instantaneous frequency $\nu(t)$.

In order to demonstrate the biomimetic modeling performance, we analyze actual dolphin and whale whistles together with our reconstructed signals using the NFM model in (3). The whistle sounds are obtained from the SOUND database of W. A. Watkins from the Woods Hole Oceanographic Institution [27]. The database provides descriptive information about each of the sound recordings. The information includes the sampling rate, record size, identification and species code of the vocalizing mammal, location of recording, and explanation on other sounds present on the recording (such as water splashes). The reconstructed NFM signal is obtained by matching the time-frequency modulation and then estimating parameters such as FM rate and duration.

In Figures 1 and 2, we compare the spectrogram TFR of an actual long-finned pilot whale whistle and its reconstructed NFM signal with $t_r = 1$. As the instantaneous frequency of the signal decreases monotonically, we reconstructed it using the hyperbolic FM signal with instantaneous frequency $c\,\nu(t) = c/t$ in Table I. As it can be seen, the time-frequency structure of the whistle and the reconstructed signal are well-matched. Similar results are shown in Figures 3 and 4 for the whistle of a white-sided dolphin using a linear FM signal; this is the signal in Table I with $t_r = 1$ and linear instantaneous frequency $\nu(t) = 2ct$. With models of cetacean mammal sounds developed using

Table I. NFM signals in (1) with $tr = 1$, nonlinear phase function and instantaneous frequency.

NFM signal	Phase function $c\,\xi(t/t_r)$	Instantaneous frequency $c\,\nu(t)$
Linear	$c\,t^2$	$2c\,t$
Hyperbolic	$c\,\ln t$	c/t
Logarithmic	$c\,t(\ln(t)-1)$	$c\,\ln t$
Power	$c\,t^{\kappa}$	$c\,\kappa\,t^{\kappa-1}$
Exponential	$c\,e^t$	$c\,e^t$

NFM, nonlinear frequency-modulated.

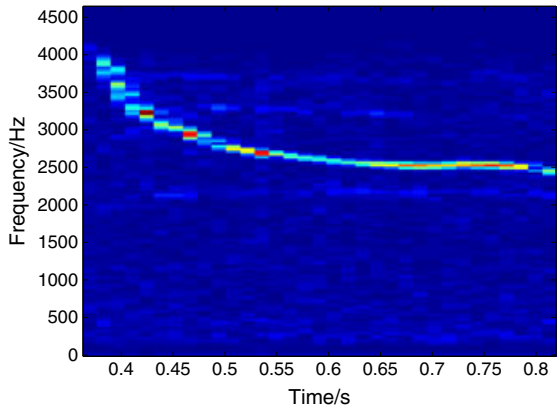

Figure 1. Spectrogram time-frequency representation of long-finned pilot whale whistle.

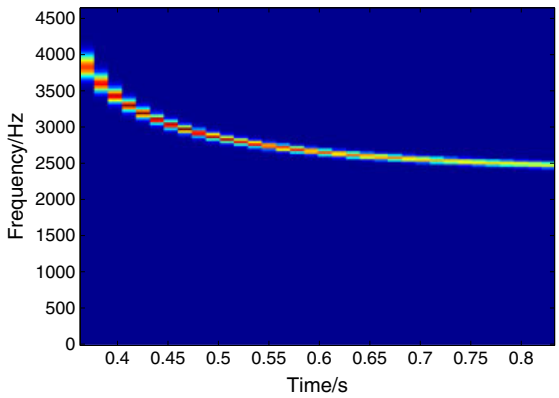

Figure 2. Spectrogram time-frequency representation of reconstructed noiseless hyperbolic FM chirp signal that best matches the time-frequency signature of the whistle.

appropriate parametrization, we can now propose a new communication scheme exploiting such sounds.

3. PROPOSED COMMUNICATION SCHEME

We propose to use a signaling scheme that uses biomimetic signals as the transmission signals that carry digital data. The structure of such signals has been already reviewed in the previous section. Such a communication system may have applications requiring LPI and LPD as the biomimetic signals sound like other natural sounds that exist in the underwater environment. Specifically, in this paper, we propose to use generalized NFM signals to model the mammal sounds. We first select NFM signals to mimic mammal whistles by matching their TF structures, we parametrize this analytical model, and we modulate these parameters with our digital data.

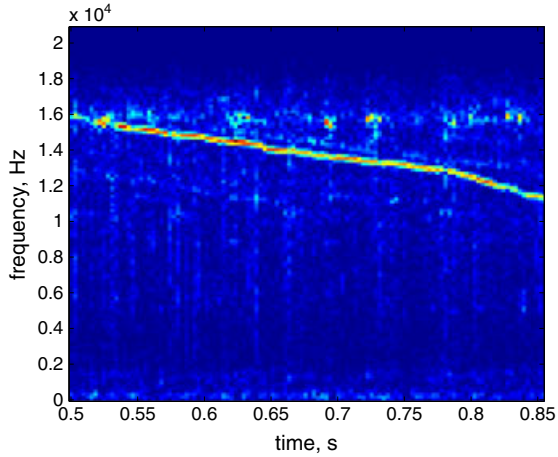

Figure 3. Spectrogram time-frequency representation of white-sided dolphin whistle.

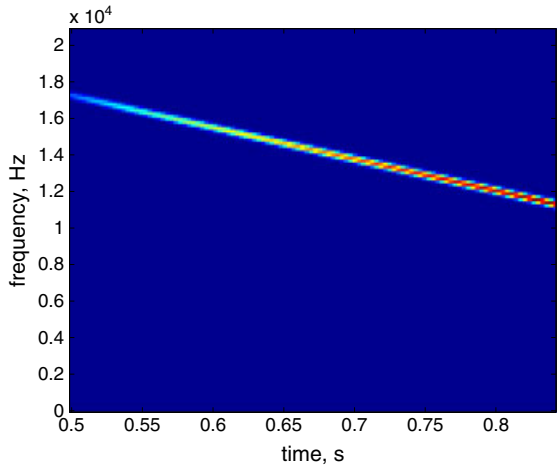

Figure 4. Spectrogram time-frequency representation of reconstructed noiseless linear FM chirp that best matches the time-frequency structure of the whistle.

The complex envelope of the acoustic NFM signal can be given in the time-domain as

$$\tilde{s}(t;\mathbf{b}) = A\alpha(t)\exp\left(j2\pi c\xi(t/t_r)\right), \qquad 0 < t \leq T_d \quad (4)$$

where $\xi(t/t_r)$ is the signal's time-varying phase function (assumed differentiable) and $t_r > 0$ is a normalization time constant. The vector parameter $\mathbf{b}$ contains information about the signal's FM rate $c \in \mathbb{R}$, duration T_d, amplitude $A \in \mathbb{R}$, and phase function $\xi(t/t_r)$. The amplitude modulation $\alpha(t)$ can be changed without affecting the TF of the whistle, and it can be used as another parameter to carry data. As we see from (4), we can use the amplitude, the carrier frequency, the FM rate, and the chirp duration as the parameters that carry our bitstream. At the receiver side, as a practical solution, we develop a maximum likelihood

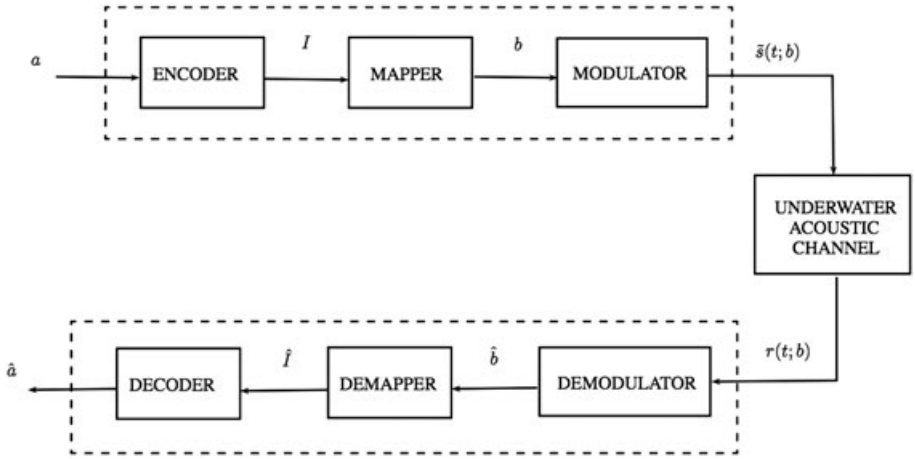

Figure 5. Block diagram of the communication system.

estimator (MLE) to estimate the value of these parameters and decode for the transmitted bits accordingly.

To summarize, a vector $\mathcal{I}$ of information bits is mapped onto the vector of parameters $\mathbf{b}$ using a certain mapping rule $f(\mathcal{I})$ that maps between the information bits into the set of signal parameters $\mathcal{C}$. There are several mapping rules that can be considered here, for example, the range of each parameter is divided into 2^n (n is the number of bits) levels then linear mapping is performed between the digital data and the parameter's levels. Then, the acoustic signal $\tilde{s}(t;\mathbf{b})$ is synthesized and transmitted over the channel. At the receiver side, we develop a detector to find an estimate $\hat{\mathbf{b}}$ of the values of these signal parameters. We use an MLE to accomplish this. Finally, a demapping function $f^{-1}\left(\hat{\mathbf{b}}\right)$ is used to restore the transmitted bits. This process is illustrated using a block diagram shown in Figure 5.

3.1. Receiver design for additive white Gaussian noise channels

In this section, we consider the use of the proposed communication scheme over an AWGN channel. We develop the MLE for the Gaussian channel, and we characterize its performance.

Given a sequence of information bits $\mathbf{a}$, we split this information sequence into words each consisting of a given number of bits. We use these consecutive words to modulate the mammal sound parameters, that is, amplitude, phase, and frequency by picking a certain value for these parameters from the set of values specified for each parameter. Upon receiving the signal at the receiver, we find an estimate for the transmitted parameters and demap these estimates into bits according to the demapping rule.

The discrete time version of a real generalized NFM is defined as

$$s[n] = A\sqrt{\nu[n]}\cos(2\pi c\xi[n]), \qquad n = 0, 1, \ldots, M-1, \tag{5}$$

where A is the amplitude of the signal, c is the generalized FM parameter that controls the shape of the instantaneous frequency, $\xi[n]$ is the phase function, $\nu[n]$ is the discrete version of the instantaneous frequency $\nu(t) = \frac{d}{dt}\xi(t)$, and M is the number of samples that corresponds to the signal duration. We consider the NFM signal in (5) as the transmitted chirp signal with parameters A, c, and M that convey the digital bits. The duration of the signal is used as a parameter such that for a fixed interval N, the signal duration varies within this N period. Thus, the received signal can be written as

$$x[n] = \begin{cases} s[n] + w[n] & \text{if } n = 0, 1, \ldots, M-1, \\ w[n] & \text{if } n = M, \ldots, N-1. \end{cases} \tag{6}$$

where $w[n]$ is the AWGN noise sample with zero mean and variance σ^2.

Before we describe the proposed receiver structure, we note that the optimal solution (to minimize the error probability) is the solution of an $M-$ary hypothesis testing problem where each of the hypotheses corresponds to a particular sequence of bits packed into the NFM signal. However, the number of bits transmitted with each packet (e.g., dolphin sound) is too many, and hence coming up with the optimal solution becomes problematic (as one would need to consider each of these M hypotheses, compute their likelihoods, and pick the one with the largest value). For instance, when there are 50 bits in a packet, there are a total of 2^{50} different hypotheses making the optimal solution impractical. Therefore, we consider a suboptimal approach to complete the receiver design: using an MLE estimator to estimate the signal parameters and then demapping the estimated values into bits.

The MLE [28] of a scalar parameter ϕ is defined as the value of the parameter that maximizes the conditional probability density function (PDF) $p(\mathbf{x};\phi)$ of the observation sequence $\mathbf{x}$. The maximization is performed over the space of the parameter ϕ. The conditional PDF of the received signal $x[n]$ defined in (6) is given by

$$p(\mathbf{x}; A, c, M) = \frac{1}{(2\pi\sigma^2)^{N/2}} \exp\left[-\frac{1}{2\sigma^2}\left(\sum_{n=0}^{M-1}\left(x[n] - A\sqrt{\nu[n]}\cos(2\pi c\xi[n])\right)^2 + \sum_{n=M}^{N-1}(x[n])^2\right)\right].$$

Thus the MLE estimate of the parameters A, c, and M is

$$\begin{bmatrix}\hat{c}\\ \hat{M}\\ \hat{A}\end{bmatrix} = \underset{\substack{c,M,A\\ c_1\le c\le c_2\\ M_1\le M\le M_2\\ A_1\le A\le A_2}}{\arg\max}\ \frac{1}{(2\pi\sigma^2)^{N/2}} \exp\left[-\frac{1}{2\sigma^2}\left(\sum_{n=0}^{M-1}\left(x[n] - A\sqrt{\nu[n]}\cos(2\pi c\xi[n])\right)^2 + \sum_{n=M}^{N-1}(x[n])^2\right)\right], \tag{7}$$

which is equivalent to

$$\begin{bmatrix}\hat{c}\\ \hat{M}\\ \hat{A}\end{bmatrix} = \underset{\substack{c,M,A\\ c_1\le c\le c_2\\ M_1\le M\le M_2\\ A_1\le A\le A_2}}{\arg\min}\ \left\{\sum_{n=0}^{M-1}\left(x[n] - A\sqrt{\nu[n]}\cos(2\pi c\xi[n])\right)^2 + \sum_{n=M}^{N-1}(x[n])^2\right\}. \tag{8}$$

This problem can be reformulated as follows:

$$\begin{bmatrix}\hat{c}\\ \hat{M}\\ \hat{A}\end{bmatrix} = \underset{M, M_1\le M\le M_2}{\arg\min}\left\{\underbrace{\min_{\substack{c,A\\ c_1\le c\le c_2\\ A_1\le A\le A_2}}\sum_{n=0}^{M-1}\left(x[n] - A\sqrt{\nu[n]}\cos(2\pi c\xi[n])\right)^2}_{\text{separate optimization problem}} + \sum_{n=M}^{N-1}(x[n])^2\right\}. \tag{9}$$

Thus, for a fixed value of M, we can separate the problem into two consecutive problems: one optimizes over the duration and the other optimizes over the other parameters (the FM rate c and amplitude A), for a specific duration. Therefore, the optimal solution (for the estimation problem) can be obtained by considering all possible values of the signal duration (determined from the particular mapping from bits to parameters adopted), performing the inner optimization for each of these values, and picking the most likely result as the optimal estimates for the three parameters embedded into the signal. Each of the inner optimization problems (optimization of A and c for a given M) involve (as we will see shortly) a one-dimensional grid search, which may be costly. Therefore, to reduce the computational burden of the algorithm, we propose the following: estimate the A and c values based on the lowest possible value for the signal duration (hence it is guaranteed that the actual signal is present in this window), and then use these estimates search over the parameter M (going over all possibilities). We adopt the latter simplification in our results section. There is another suboptimal solution that can be considered to solve the optimization problem in (9) using a simple energy detector followed by a decoder that estimates the other parameters; in other words, changing the order at which the parameters are estimated. Our experimental results show that there is no significant difference on the system performance by changing the order in which the parameters get estimated, that is, both simplifications result in similar performance.

For a given duration $\tilde{M}$, we define $r[n] = \sqrt{\nu[n]}\cos(2\pi c\xi[n])$, $n = 0, \ldots, \tilde{M} - 1$, and the vector of parameters θ

$$\theta = \begin{bmatrix}A\\ c\end{bmatrix}. \tag{10}$$

The cost function $g(A, c; \tilde{M})$ is defined as

$$g\left(A, c; \tilde{M}\right) = \sum_{n=0}^{\tilde{M}-1}\left(x[n] - A\sqrt{\nu[n]}\cos(2\pi c\xi[n])\right)^2, \tag{11}$$

$$= \sum_{n=0}^{\tilde{M}-1}(x[n] - Ar[n])^2. \tag{12}$$

Thus, the solution to the MLE problem is reduced to

$$\hat{\theta} = \underset{\substack{c,A\\ c_1\le c\le c_2\\ A_1\le A\le A_2}}{\arg\min}\ g\left(A, c; \tilde{M}\right). \tag{13}$$

To estimate the parameters A and c, we need to do a two-dimensional grid search over the given range of both parameters. However, this two-dimensional search can be

reduced to a one-dimensional one instead as we are able to find a closed form expression for the optimal estimator of the amplitude given any value of c. That is, for each value of c, the optimal amplitude parameter value can be found by solving the following optimization problem

$$\hat{A} = \underset{A:A_1 \le A \le A_2}{\arg\min} \sum_{n=0}^{\tilde{M}-1} (x[n] - Ar[n])^2, \tag{14}$$

with the Lagrangian is given by

$$L(A, \lambda_1, \lambda_2) = \sum_{n=0}^{\tilde{M}-1} (x[n] - Ar[n])^2 + \lambda_1(A - A_2) - \lambda_2(A - A_1). \tag{15}$$

The resulting Karush-Kuhn-Tucker (KKT) conditions are then

$$-2\sum_{n=0}^{\tilde{M}-1} (x[n] - Ar[n])r[n] + \lambda_1 - \lambda_2 = 0, \tag{16}$$

$$\lambda_1 \ge 0, \quad \lambda_2 \ge 0, \quad \lambda_1(A - A_1) = 0, \quad \lambda_2(A - A_2) = 0. \tag{17}$$

If we define $\hat{A} = \underset{A}{\arg\min} \sum_{n=0}^{\tilde{M}-1} (x[n] - Ar[n])^2$, then, an optimal solution for the problem is

$$A^* = \begin{cases} \hat{A} & \text{if } A_1 \le \hat{A} \le A_2, \\ A_1 & \text{if } \hat{A} < A_1, \\ A_2 & \text{if } \hat{A} > A_2. \end{cases} \tag{18}$$

We now study the asymptotic behavior of the MLE for the parameters A and c. Under certain regularity conditions [29], the MLE has asymptotically (as the number of samples become large) a Gaussian distribution with mean being the true mean and covariance matrix given by the inverse of the Fisher information matrix [28]. Theseregularity conditions include the following: the true parameter value must be interior to the parameter space, the log-likelihood function must be twice differentiable, the second derivatives must be bounded, and the expected value of the log-likelihood function must equals zero when the values of the parameters are taken as the true values. It is straightforward to show that the MLE of the vector θ in our case satisfies these conditions, and hence, for large number of samples, the estimated vector of parameters $\hat{\theta}$ has a Gaussian distribution

$$\hat{\theta} \sim \mathcal{N}\left(\theta, I(\theta)^{-1}\right), \tag{19}$$

where $I(\theta)^{-1}$ is the Fisher Information matrix derived in Appendix A.

3.2. Receiver design for time-varying multipath channels

We now consider the case of transmission over a time and frequency dispersive channel, which is typical in UWA communications. In this case, the discrete time received signal can be written as

$$x[n] = \begin{cases} \sum_{l=0}^{L-1} h_l[n]s[n-l] + w[n] & \text{if } n = 0, 1, \ldots, M-1, \ldots, M+L-2, \\ w[n] & \text{if } n = M+L-1, \ldots, N-1. \end{cases} \tag{20}$$

where $w[n]$ is an AWGN, and $h_l[n]$ is the time-varying channel coefficient for the lth delay pin at the nth instant. We assume that the receiver has an estimate for these channel coefficients. In practice, the time-varying channel taps can be estimated with some accuracy using known transmitted bits (pilot bits). To accomplish this, we can use one of the common channel estimation techniques for UWA channels, for example, the matching pursuit (MP) [30,31] or basis pursuit (BP) [32] algorithms.

The PDF of the received signal for a given set of parameters A, c, and M is given by

$$p(\mathbf{x}; A, c, M) = \frac{1}{(2\pi\sigma^2)^{N/2}} \exp\left[-\frac{1}{2\sigma^2}\left(\sum_{n=0}^{M-1}\left(x[n] - A\sum_{l=0}^{L-1} h_l[n]r[n-l]\right)^2 + \sum_{n=M}^{N-1}(x[n])^2\right)\right]. \tag{21}$$

Thus, the MLE problem can be written as

$$\begin{bmatrix} \hat{c} \\ \hat{M} \\ \hat{A} \end{bmatrix} = \underset{\substack{c,M,A \\ c_1 \le c \le c_2 \\ M_1 \le M \le M_2 \\ A_1 \le A \le A_2}}{\arg\max} \frac{1}{(2\pi\sigma^2)^{N/2}} \exp\left[-\frac{1}{2\sigma^2}\left(\sum_{n=0}^{M-1}\left(x[n] - A\sum_{l=0}^{L-1} h_l[n]r[n-l]\right)^2 + \sum_{n=M}^{N-1}(x[n])^2\right)\right], \tag{22}$$

where $r[n] = \sqrt{\nu[n]}\cos(2\pi c\xi[n])$, $n = 0, \ldots, M-1$.

Let us define $u[n] = \sum_{l=0}^{L-1} h_l[n]r[n-l]$, $n = 0, \ldots, M$. Thus, the maximization defined before is equivalent to

$$\begin{bmatrix} \hat{c} \\ \hat{M} \\ \hat{A} \end{bmatrix} = \underset{\substack{c,M,A \\ c_1 \le c \le c_2 \\ M_1 \le M \le M_2 \\ A_1 \le A \le A_2}}{\arg\min} \left\{ \sum_{n=0}^{M-1} (x[n] - Au[n])^2 + \sum_{n=M}^{N-1} (x[n])^2 \right\}, \tag{23}$$

which can be reformulated as

$$\begin{bmatrix} \hat{c} \\ \hat{M} \\ \hat{A} \end{bmatrix} = \underset{M:M_1 \le M \le M_2}{\arg\min} \left\{ \underbrace{\min_{c,A} \sum_{n=0}^{M-1} (x[n] - Au[n])^2}_{\text{separate optimization problem}} + \sum_{n=M}^{N-1} (x[n])^2 \right\}. \tag{24}$$

To perform the inner optimization for each value of M, as in the previous case, we perform a one-dimensional grid search (over the parameter c) instead of the two-dimensional grid search over the two parameters A and c because we are able to find the optimal estimator for the amplitude given the value of c. For a given value of the signal duration and the c value, the optimal solution for the amplitude estimate is

$$\hat{A} = \frac{\sum_{n=0}^{\hat{M}} x[n]u[n]}{\sum_{n=0}^{\hat{M}} u^2[n]}. \tag{25}$$

Therefore, the optimal MLE can be obtained similar to the one in the previous section. As an alternative, to simplify the solution, we can estimate the parameters A and c for the lowest possible value of the signal duration and then search over the possible signal durations using these estimated quantities. This is the approach adopted in the examples section.

As in the previous subsection, the asymptotic distribution of the MLE estimated vector $\hat{\theta}$ is Gaussian with mean equal to the true mean and covariance matrix given by the inverse of the Fisher information matrix, that is

$$\hat{\theta} \sim \mathcal{N}\left(\theta, I(\theta)^{-1}\right), \tag{26}$$

where $I(\theta)^{-1}$ is the Fisher Information matrix derived in Appendix B.

4. ERROR PROBABILITY ANALYSIS

In the previous section, we have argued that the estimated parameter vector in our digital communication system can be modeled as

$$\hat{\theta} = \theta + \rho, \tag{27}$$

where $\hat{\theta}$ is a vector of the estimated parameters, θ is a vector of the actual parameter values, and ρ is a Gaussian-distributed noise vector with zero mean and covariance matrix given by the inverse of the Fisher information matrix. This is a common channel model, and there are many standard techniques that can be used to analyze the bit error probability (BEP) of the proposed system. For instance, we can resort to the union bound on the BEP.

In our proposed communication scheme, the acoustic signal that is being transmitted has n parameters that convey the digital bits; these signal parameters take values from their given range. Thus, every transmitted acoustic signal is synthesized by picking a combination from these parameters. An equivalent model for the system is derived from the analysis of the asymptotic ML estimator of the signal parameters in (19). In this equivalent model, the received signal can be represented as an n-dimensional vector of parameters that are transmitted over an additive colored Gaussian noise. Hence, we can use noise whitening and apply the standard union bound to estimate the error rates.

We now give a specific (toy) example to demonstrate the performance of the proposed communication system. We use a hyperbolic signal with two parameters used for the modulation purposes, namely, the amplitude A and the FM rate c. We transmit the signal $x(t)$

$$x(t) = A\sqrt{v(t)}\cos(2\pi c\xi(t)), \quad 0 < t < T, \tag{28}$$

where $\xi(t) = \ln(t)$ and $v(t) = \frac{d\eta(t)}{dt} = \frac{1}{t}$. In this example, T is the signal duration taken as 10 ms and A and c are the parameters that are used to carry the information bits. The value of the parameter A ranges between 1 and 8, and c ranges between 20 and 22 kHz. Each parameter is quantized into five bits. Thus, the size of the two-dimensional signal constellation is 1024 points. Figure 6 shows the BEP of the proposed communication scheme, using Monte Carlo simulations, and the union bound computed using

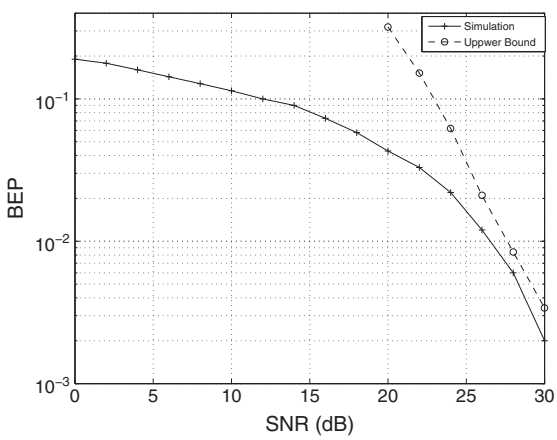

Figure 6. Simulated bit error probability (BEP) and union bound.

the approach in the previous paragraph. It is clear that the union bound on the BEP matches the BEP computed from the simulations well for high SNR.

5. EXPERIMENTAL RESULTS

We now provide some experimental results for the proposed communication system based on measurements taken at the recent KAM11 experiment [33].

5.1. Kauai Acomms MURI 2011 Experiment

The KAM11 experiment was conducted in shallow water off the western coast of Kauai, Hawaii, at the Pacific Missile Range Facility during the period 23 June and 12 July 2011. The bathymetry of the operation area is shown in Figure 7. We consider a fixed-source scenario at which there is no intentional motion between the transmitter and the receiver. The positions of the adopted transmitters and receivers are illustrated in Figures 8 and 9. An eight-element vertical-array source was deployed with an inter-element separation of 7.5 m and an aperture of 52.5 m. The top element was at a nominal depth of 30 m, and the bottom element was not anchored to the sea floor. At the receiver side, a 16-element vertical array was deployed at a distance of 3 km from the source. The inter-element spacing was 3.75 m, with the top element deployed at a nominal depth of 35.5 m.

The transmitted signal is a linear FM signal $x(t)$, given by

$$x(t) = A\cos(2\pi f_0 t + 2\pi c t^2), \qquad 0 < t < T \qquad (29)$$

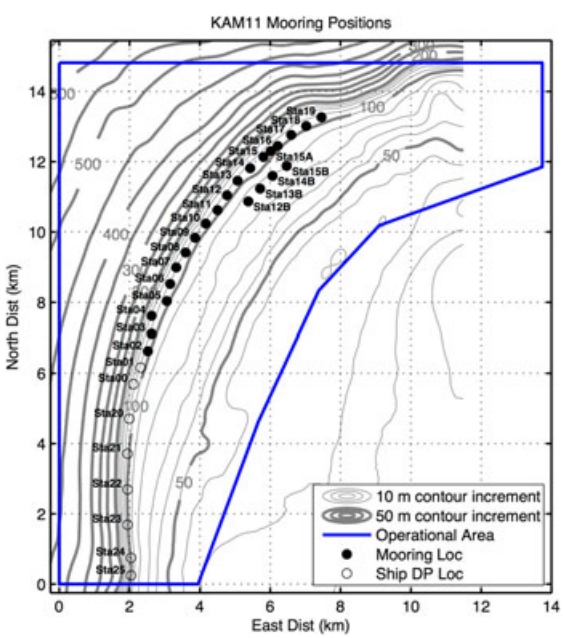

Figure 7. The operation area in the Kauai Acomms MURI 2011 (KAM11) (taken from [33]).

where A is the amplitude of the signal, f_0 is the center frequency, c is the FM rate, and T is the signal duration. The amplitude was then between 0.5 and 1; the center frequency was between 22 kHz and 26 kHz; the FM rate was changed between 2 kHz and 10 kHz, and the signal duration was selected from 100 ms to 200 ms. Each parameter is quantized into 4 to 10 bits to obtain different transmission rates. We note that the transmission parameters (frequency bands of operation, etc.) are selected based on the requirements of the available hardware during the KAM11 experiment. This should be taken as a proof of concept that demonstrates the working principles of the proposed communication set-up and its viability in providing low error rates. In a real application requiring LPI/LPD, the parameters can be selected according to the mammal sound models provided in Section 2.2.

We further note that, according to the biomimetic signal model in (1), $\alpha(t)$ should be chosen as $\sqrt{\left|\frac{d}{dt}\xi(t)\right|}$ to guarantee the orthogonality of the transmitted signals. However, in our experiment, and for the sake of simplicity, we choose $\alpha(t) = 1$. Hence, the orthogonality of the transmitted signal is no longer guaranteed, which deteriorates the resulting performance. On the other hand, the experimental results show that we are still able to successfully decode the transmitted bits with a relatively low bit error rate, which suggests the robustness of the proposed communication scheme.

Every recoding consists of seven transmission frames (sometimes, called subgroups), where each subgroup corresponds to a different transmission rate. These different rates are attained from the fact that we map each parameter to different number of bits, for example, in the first subgroup, the parameters are mapped to four bits, in the second subgroup, the parameters are mapped to five bits and so on. In each subgroup, we transmit 30 consecutive chirp sequences separated by a 60 ms guard period. Thus, the transmission rates that correspond to these subgroups are 107, 127, 147, 167, 187, 207, and 227 bps, respectively. In Section 5.4, we will present decoding results obtained for these different rates using different receiver combining techniques.

During the experiment, the transmitter/receiver separation was about 3 km. Defining the SNR at the receiver as the ratio between the signal power and the noise power after the amplifier and the bandpass digital filter, the corresponding SNR during the transmission is estimated to be around 11 dB. Because the SNR observed during the experiment was relatively high, we also consider decoding of the experimental data at lower SNRs by adding artificial (Gaussian) noise to the observations. Figure 10 shows the bit error rate (BER) versus the SNR for different transmission rates, which are obtained by using majority voting combining technique (will be discussed later in more details) across the 16-antenna elements. It is clear that it is possible to decode the transmitted data with a reasonable BEP even at very low SNR values.

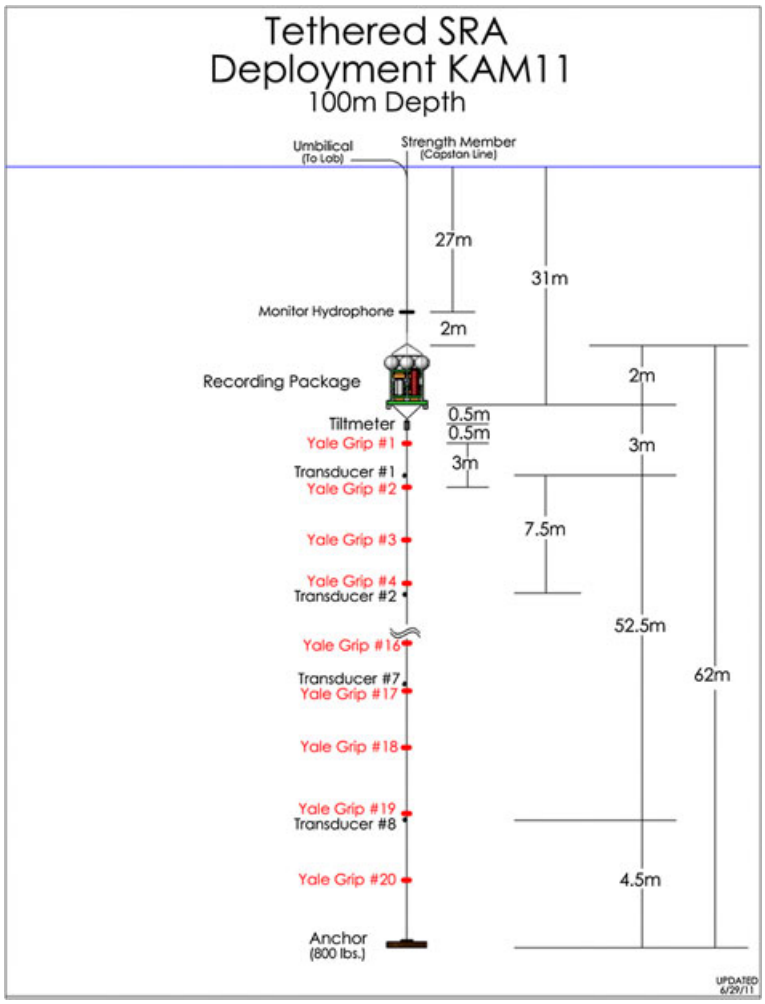

Figure 8. The positions of the adopted transmitters (taken from [33]). KAM11, Kauai Acomms MURI 2011.

5.2. Channel estimation

For the channel estimation purposes, we use the transmitted linear FM signals as the channel probes. We employ the MP algorithm [31] to find an estimate of the channel coefficients. The MP algorithm is based on synthesizing a signal dictionary that consists of the transmitted signal and delayed versions of this signal. Because the power spectral density of linear FM signals is not close to white, a resolution issue appears in the channel estimation process as signal cannot resolve all the arrivals that lie in a certain time interval. Nevertheless, we are constrained to using these signals as channel probes as no other signals were transmitted during the experiment. As an example, Figure 11 shows the power spectral density of a linear FM signal. In other words, we cannot use a dictionary with a high resolution, and we have to settle for a coarse channel estimate. Even with this coarse channel estimate, we are able to report acceptable raw error probabilities; hence, this is not a major issue.

For the MP algorithm, due to the correlation structure of the transmitted signal, we use a dictionary that allows us to resolve only paths within 1 ms separation. The stopping criteria we set for the MP algorithm are the number of resolvable paths identified. We stop the algorithm when the number of resolvable paths equals 20, which means that we are able to span a delay spread of about 20 ms.

As an example, Figure 12 shows the time-varying channel impulse response, which is computed over a duration equals to the duration spanned by 30 adjacent signals. These channel responses correspond to the channel between the transmitter and the first receive element. From these figures, we can notice that the channel does not significantly change from signal block to the other. The reason that we observe a slowly varying channel is because of our channel estimator being a coarse one. The channel in KAM 2011 at a finer resolution changes more significantly as reported in [33]. For instance, we see in Figure 14(b) on page 34 and Figure 15(b) on page 35 in [33] that the change in the channel taps within a second or less is because of slight change in the arrival time—which is not being

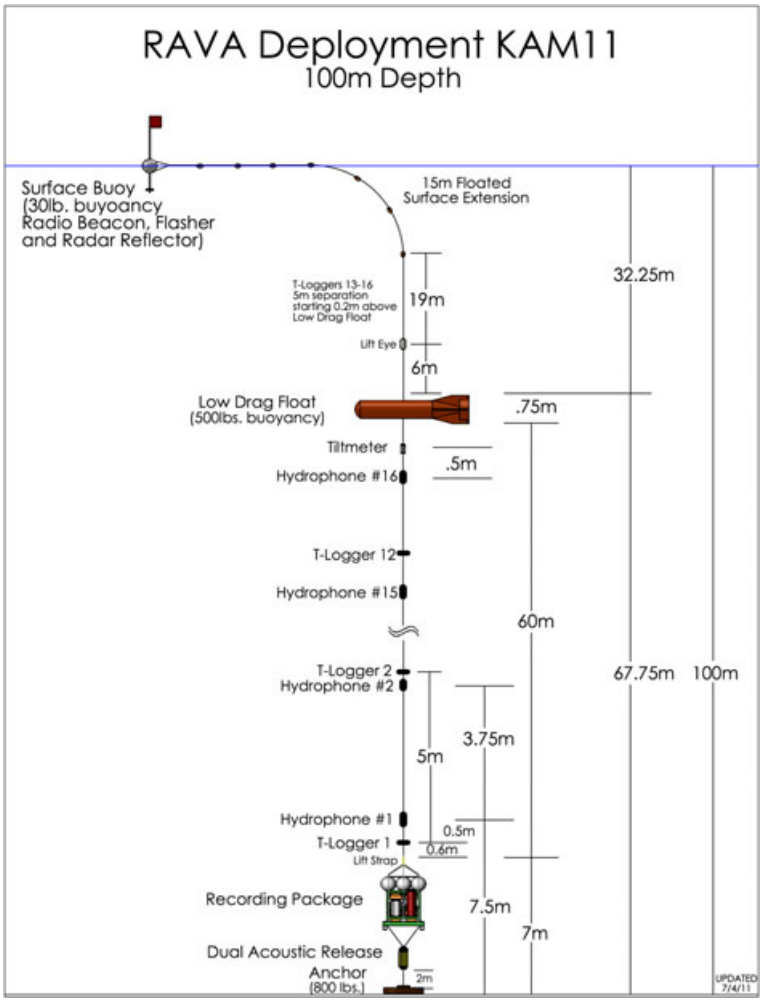

Figure 9. The positions of the adopted receivers (taken from [33]). KAM11, Kauai Acomms MURI 2011.

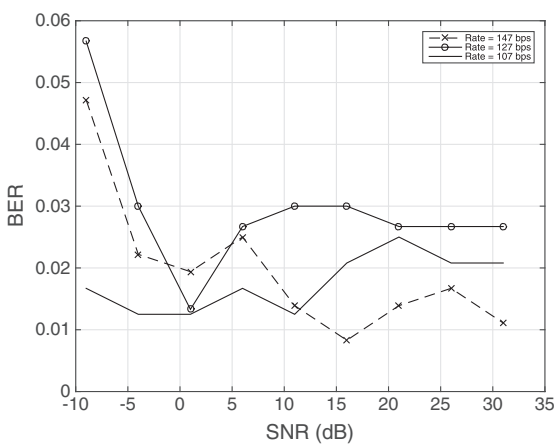

Figure 10. Bit error rate (BER) as a function of the SNR (emulated by adding Gaussian noise on the recorded data).

resolved in our channel estimates (being obtained from linear FM signals as opposed to OFDM or other probe signals with a high resolution). This observation (on the estimated channel being slowly varying) will help us in the decoding process as we will see later.

5.3. Receiver structure

The receiver has 16 elements, therefore it is possible to use receive diversity to enhance the performance of the system. During our investigations, we explore different combining techniques that can be used. The decoding process works as follows: we use the MLE to find estimates of the signal parameters at each receive element, then we decode these parameters into bits according to the mapping rule used at the transmitter side. Then, we apply a diversity combining technique to combine the decoded bits across all the receive elements. In the following subsections, we summarize the different combining techniques we use.

5.3.1. Majority voting combining.

In the majority voting (MV) combining technique, the final decision is made by the majority voting rule. In other

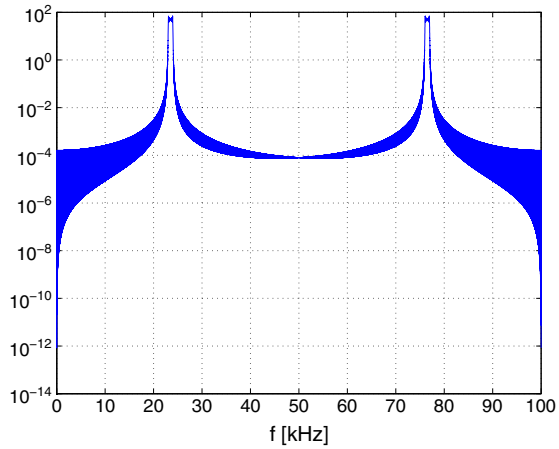

Figure 11. Power spectral density function of a linear FM signal.

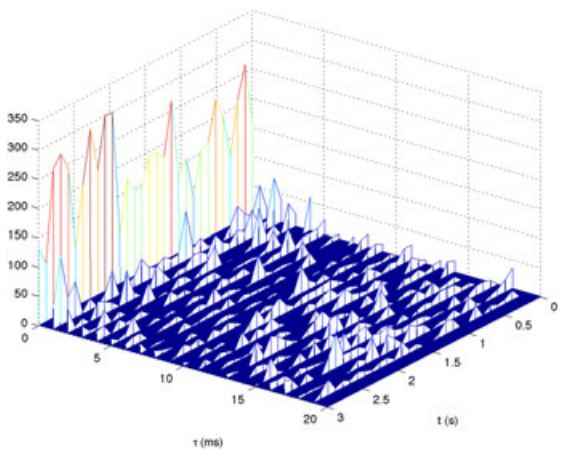

Figure 12. Channel impulse response for 30 consecutive linear FM signals at the first receive element (these estimates have been computed from the data recorded on 2 July 2011 at 3:24 during the Kauai Acomms MURI 2011 experiment).

words, the final decision is said to be "1" if more than half of the receive elements decide for "1" and vice versa.

5.3.2. Weighted sum combining.

In weighted sum (WS) combining schemes, the overall rule is based on weighting each receive element with a certain weight based on the reliability of its decision. We propose to use two different weighting schemes based on the model of the decoded bits. The first model is derived from the asymptotic behavior of the MLE. We know that the PDF of the estimated parameters is Gaussian with means equal the true value and the variance computed from the inverse of the Fisher information matrix. So, for the ith receive element, we have

$$\eta_i \sim \mathcal{N}(\eta_0, I_i(\eta_0)^{-1}), \tag{30}$$

where η_0 is the true value. In our case, the vector of parameters η is given by

$$\eta = \begin{bmatrix} C \\ F_0 \end{bmatrix}. \tag{31}$$

Thus, MLE of the mean η_0 is

$$\hat{\eta}_0 = \left(\sum_{i=0}^{N_r-1} I_i(\hat{\eta}_i) \right)^{-1} \sum_{i=0}^{N_r-1} I_i(\hat{\eta}_i)\, \eta_i, \tag{32}$$

where N_r is the number of the receive elements at the receiver and $\hat{\eta}_i$ is the estimate of the vector of parameters η at the ith receiver element.

The second WS combining technique we use is based on the classical maximum ratio combining model. In this scheme, the output bit from the ith receive element is modeled as

$$d^{(i)} = \alpha^{(i)} q + n^{(i)}, \tag{33}$$

where q is the original transmitted bit, $\alpha^{(i)}$ is the ℓ^2-norm of the estimated channel vector $\mathbf{h}^{(i)}$ at the ith receive element, and $n^{(i)}$ is the additive noise at the ith receive element. Thus, the weight of the output bit at the ith receive element is

$$\gamma_i = \frac{\left|\alpha^{(i)}\right|^2}{\hat{\sigma}_i^{\,2}}, \tag{34}$$

where $\hat{\sigma}_i^{\,2}$ is the noise variance at the ith receive element. We measure the noise variance from the silence period that exist between the transmission blocks using

$$\hat{\sigma}^2 = \frac{1}{N_s} \sum_{n=0}^{N_s-1} x[n]^2, \tag{35}$$

where N_s is the length of the silence period and $x[n]$ is the received signal at the nth instant. We define the vector $\boldsymbol{\gamma} = \left[\gamma_1, \gamma_2, \ldots, \gamma_{N_r}\right]^T$, and we combine the soft values of the bits as follows

$$d_{combined} = \frac{1}{||\boldsymbol{\gamma}||_1} \boldsymbol{\gamma}^T \mathbf{d}, \tag{36}$$

where $||\cdot||_1$ denotes ℓ_1-norm. This combined value $d_{combined}$ is used with a threshold to make the final decision, the value of this threshold is $\frac{1}{2}$ as we assume the same a priori probabilities for "0" and "1."

5.3.3. Selection combining.

The last combining technique used is the selection combining (SC). In this case, we perform the selection based on the two models described before. For the first model, we select the decision made by the receive element that has the lowest noise variance. For the FM rate c, we choose the decision made by the element l_c, which is given by

$$l_c = \arg\min_i \sigma^2_{c^{(i)}}, \tag{37}$$

and for the frequency f_0, we choose the decision made by the element l_{f_0}, which is given by

$$l_{f_0} = \arg\min_i \sigma^2_{f_0^{(i)}}. \tag{38}$$

5.4. Decoding results

We now present BER results for our proposed communication scheme. At the receiver, a linear FM signal block is used to estimate the channel; then, this channel estimate is used to decode the next block, and so on. We can justify this from Figure 12 that shows that the channel impulses responses separated by a signal duration are close to each other and the channel does not change significantly from one signal block to the other. We use the 16 receive elements at the receiver to decode the linear FM parameters. Table II shows the uncoded error probability of the parameters for the three combining techniques described before. We show the error probability results for 19 different recordings. The results correspond to a transmission rate of 107 bps. These recordings were taken on 2 July 2011 at 3:24, 5:24, 7:24, 9:24, 11:24, 13:24, 15:24, 17:24, 19:24, 21:24, and 23:24, respectively, and on 3 July 2011 at 3:24, 5:24, 7:24, 9:24, 11:24, 13:24, 17:24, 21:24, 23:24, respectively. As another example, Table III shows the error probability for different transmission rates using the MV combining technique. Figure 13 shows the BER for different parameters separately.

From the decoding results, it is clear that we are able to decode the signal parameters successfully with a good BER. Our results indicate that the amplitude and the signal duration parameters are more vulnerable to errors than the frequency and FM rate. This is expected because the UWA channel is highly dispersive and it affects the amplitude and the signal duration more than the other parameters. Also, the WS technique with the Gaussian model shows an average BER better than the other combining techniques. However, sometimes the MV shows a better BER than the WS. We have observed that the SC technique shows the worst performance among all the techniques (we did not show the resulting decoding error for that technique). Also, by comparing the two models of the WS technique, we can notice that the first model (the Gaussian one) shows a better average performance than the other model.

From the decoding results of different transmission rates, we can notice that for lower data rates, the BER

Table II. The uncoded percentage error probability of the linear FM parameters for transmission rate 107 bps. The table shows the uncoded BER (in percentage) for the three combining techniques, MV and WS (two versions).

Env.	MV	WS, 1st model	WS, 2nd model
1	1.67	2.5	1.67
2	0	0	0.83
3	0	1.25	2.5
4	2.5	2.08	3.33
5	0.42	2.08	1.25
6	1.67	2.5	1.67
7	2.92	3.33	3.75
8	2.92	2.5	1.67
9	0.83	0.42	0.83
10	3.33	3.33	3.75
11	0.42	1.25	1.25
12	0	0	0.42
13	1.25	0	0.42
14	2.92	2.92	4.17
15	1.25	0.42	1.25
16	1.25	4.17	3.33
17	0	0	0
18	2.08	1.25	1.67
19	0	0	0

BER, bit error rate; MV, majority voting; WS, weighted sum.

Table III. Percentage error probability for different transmission rates using the MV combining technique.

	Rate (bps)	107	127	147	167	187	207	227
Env. 1	Error probability	1.67	3.67	2.22	1.67	5.63	8.15	13.5
Env. 2	Error probability	0	0	1.94	2.86	4.37	8.33	11.67
Env. 3	Error probability	0	2	1.11	0.71	6.54	7.41	13
Env. 4	Error probability	2.5	7	1.11	1.9	7.71	8.33	13.5

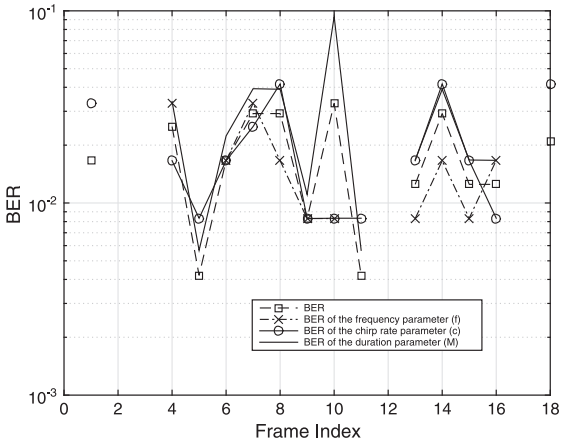

Figure 13. The bit error rate (BER) for different parameters. "Blank space" means that no error for that frame is observed. The average error rate of the frequency parameter is 0.92%, the average error rate of the FM rate parameter is 1.62%, and the average BER of the signal duration parameter is 2.17%.

is not monotonically increasing with the rate. However, for higher rates, the BER states to follow a monotonically increasing behavior (increasing the rate results on increasing the BER) as it is expected.

Although it is not our major focus, we would also like to comment on the data rates obtained in our work compared with some other work reported on covert UWA communications. In [15], the authors present results from the SPACE'08 experiment during which DSSS technique was used for data transmission (to provide covertness). The transmitter/receiver separations in this experiment are 60 m, 200 m, and 1 km. The transmit bandwidth is 7.8125 kHz that leads to a payload data rate of 156.25 bps. In this paper, we have demonstrated successful decoding results up to 207 bps over a bandwdith of 10 kHz with a transmitter/receiver separation of about 3 km (significantly longer than the ones in [15]). In [17], the authors use the duration between dolphin clicks to convey digital bits. In their work, the data rate obtained is 37 bps with transmitter/receiver separation of about 2 km, which is a lower rate than what we have demonstrated over a longer transmitter/receiver separation in this paper. We further note that we were not very aggressive in selecting the transmission rates; we anticipate that it would have been possible to pack more bits and decode them successfully or even use other set of parameters (using a different chirp signal) to carry more bits.

5.5. Interference analysis

In this subsection, we study the effects of the other coexisting mammal sounds on the system performance. We conduct our study by simple method of emulation for the KAM11 experiment. Specifically, we generate synthesized mammal sounds using the signal models described in Table I and add it to the recorded data during the KAM11 experiment. For that purpose, we assume the following: the receiver does not know the existence of the interference and we use the decoder described in Section 5.3, and the parameters of the interfering signal is random but fixed during the experiment. We consider two interference scenarios cause by two different sound signals. The first one is the hyperbolic FM signal, which is given by

$$i[nT_s] = A\sqrt{c/nT_s}\cos(2\pi c \ln nT_s + 2\pi f_0 nT_s). \quad (39)$$

Table IV shows the signal parameters that were used in the emulation. The parameters are chosen such that the interfering signal is located in the same frequency band of the transmitted signal with the maximum spread over this band, and there is severe interference. Figure 14 shows the BER for different values of signal-to-interference plus noise ratios (SINRs). The figure shows that the BER changes by no more than 1%.

The second interference model we consider is the logarithmic FM signal, which is given by

$$i[nT_s] = A\sqrt{c \ln nT_s}\cos(2\pi c n T_s(\ln nT_s - 1) + 2\pi f_0 nT_s). \quad (40)$$

Table V shows the signal parameters that have been used in the emulation. Figure 15 shows the resulting BER. From (14) and (15), we can notice that the proposed scheme shows an immunity against interference from other interfering signals.

Table IV. Signal parameters of the hyperbolic FM interfering signal.

	f_0	c	T
SINR = 8 dB	25 kHz	2 kHz	260 msec
SINR = 4 dB	25 kHz	2 kHz	260 msec

SINR, signal-to-interference plus noise ratio.

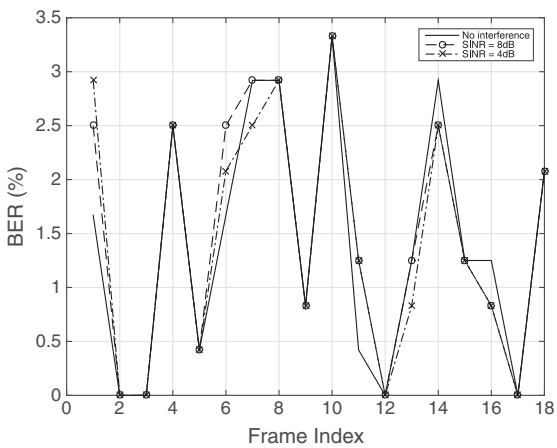

Figure 14. Bit error rates (BERs) for different values of signal-to-interference plus noise ratios (SINRs), the interfering signal is a hyperbolic FM.

Table V. Signal parameters of the logarithmic FM interfering signal.

	f_0	c	T
SINR = 9 dB	25 kHz	500 Hz	260 msec
SINR = 6 dB	25 kHz	500 Hz	260 msec

SINR, signal-to-interference plus noise ratio.

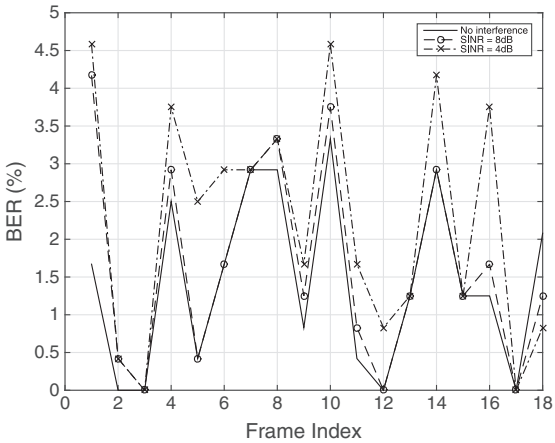

Figure 15. Bit error rates (BERs) for different values of signal-to-interference plus noise ratios (SINRs), the interfering signal is a logarithmic FM.

6. CONCLUSIONS

In this paper, we propose a new approach to UWA communications using biomimetic signals as the communication signals, where we modulate the parameters of the sound signal with information bits. We first develop analytical signal models with nonlinear instantaneous frequencies matching mammal sound signatures in the time-frequency plane. Then, we parametrize the developed signal model and use these parameters to carry information bits by mapping them to the set of parameters. We use these parameters to generate the signal to be transmitted. At the receiver side, we design an estimator to obtain the parameters of the transmitted signal and demap the estimated values to information bits. We demonstrate the viability of the proposed communication scheme via experimental results recorded at the KAM11 experiment.

APPENDIX A: FISHER INFORMATION MATRIX FOR MLE OF SIGNAL PARAMETERS TRANSMITTED ON AWGN

For a given value of the transmitted sequence length M (treated as known in the sequel), we have

$$\begin{aligned} x[n] &= s[n] + w[n] \\ &= A\sqrt{\nu[n]}\cos(2\pi c\xi[n]) + w[n], \\ n &= 0, 1, \ldots, M-1 \end{aligned} \tag{A.1}$$

We define the likelihood function for the parameters θ as

$$\begin{aligned} \ln p = \ln p(\mathbf{x};\theta) = &-\frac{M}{2}\ln\left(2\pi\sigma^2\right) \\ &-\frac{1}{2\sigma^2}\sum_{n=0}^{M-1}(x[n]-Ar[n])^2. \end{aligned} \tag{A.2}$$

The ijth element of the Fisher information matrix [28] is defined as

$$[I(\theta)]_{ij} = -\mathbf{E}\left[\frac{\partial \ln p}{\partial\theta_i}\frac{\partial \ln p}{\partial\theta_j}\right]. \tag{A.3}$$

From (A.2), we can write the following:

$$\frac{\partial \ln p}{\partial A} = \frac{1}{\sigma^2}\sum_{n=0}^{M-1}(x[n]-Ar[n])r[n], \tag{A.4}$$

$$\frac{\partial \ln p}{\partial c} = \frac{1}{\sigma^2}\sum_{n=0}^{M-1}(x[n]-Ar[n])A\frac{\partial r[n]}{\partial c}, \tag{A.5}$$

$$\frac{\partial^2 \ln p}{\partial^2 A} = -\frac{1}{\sigma^2}\sum_{n=0}^{M-1}(r[n])^2, \tag{A.6}$$

$$\begin{aligned} \frac{\partial^2 \ln p}{\partial^2 c} = \frac{1}{\sigma^2}\sum_{n=0}^{M-1}\Bigg(&-A^2\left(\frac{\partial r[n]}{\partial c}\right)^2 \\ &+(x[n]-Ar[n])A\frac{\partial^2 r[n]}{\partial^2 c}\Bigg), \end{aligned} \tag{A.7}$$

$$\begin{aligned} \frac{\partial^2 \ln p}{\partial A\partial c} = \frac{1}{\sigma^2}\sum_{n=0}^{M-1}\Bigg(&-A\left(\frac{\partial r[n]}{\partial c}\right)r[n] \\ &+(x[n]-Ar[n])\frac{\partial r[n]}{\partial c}\Bigg), \end{aligned} \tag{A.8}$$

$$\frac{dr[n]}{dc} = -2\pi\xi[n]\sqrt{\nu[n]}\sin(2\pi c\xi[n]), \tag{A.9}$$

and since $\mathrm{E}[(x[n]-Ar[n])] = 0$, we obtain

$$[I(\theta)]_{11} = -\mathrm{E}\left[\frac{\partial^2 \ln p}{\partial^2 A}\right] = \frac{1}{\sigma^2}\sum_{n=0}^{M-1} r^2[n],$$

$$[I(\theta)]_{12} = -\mathrm{E}\left[\frac{\partial^2 \ln p}{\partial A\partial c}\right] = \frac{1}{\sigma^2}\sum_{n=0}^{M-1}\left(Ar[n]\frac{\partial r[n]}{\partial c}\right),$$

$$[I(\theta)]_{21} = [I(\theta)]_{12},$$

$$[I(\theta)]_{22} = -\mathrm{E}\left[\frac{\partial^2 \ln p}{\partial^2 c}\right] = \frac{1}{\sigma^2}\sum_{n=0}^{M-1}\left(A\frac{\partial r[n]}{\partial c}\right)^2.$$

APPENDIX B: FISHER INFORMATION MATRIX FOR MLE OF SIGNAL PARAMETERS TRANSMITTED ON MULTIPATH CHANNELS

Given the transmitted sequence length M, we have

$$x[n] = \begin{cases} \sum_{l=0}^{L-1} h_l[n]s[n-l] + w[n] & \text{if } n = 0, 1, \ldots, M-1, \ldots, M+L-2 \\ w[n] & \text{if } n = M+L-1, \ldots, N-1. \end{cases} \tag{B.1}$$

similar to the AWGN case, the likelihood function for the vector θ for a given M is

$$\ln p(\mathbf{x}; \theta) = -\frac{M}{2} \ln\left(2\pi\sigma^2\right) - \frac{1}{2\sigma^2} \sum_{n=0}^{M-1} (x[n] - Au[n])^2. \tag{B.2}$$

Also

$$\frac{\partial \ln p}{\partial A} = \frac{1}{\sigma^2} \sum_{n=0}^{M-1} (x[n] - Au[n])u[n], \tag{B.3}$$

$$\frac{\partial \ln p}{\partial c} = \frac{1}{\sigma^2} \sum_{n=0}^{M-1} (x[n] - Au[n])A \frac{\partial u[n]}{\partial c}, \tag{B.4}$$

$$\frac{\partial^2 \ln p}{\partial^2 A} = -\frac{1}{\sigma^2} \sum_{n=0}^{M-1} u^2[n], \tag{B.5}$$

$$\begin{aligned} \frac{\partial^2 \ln p}{\partial^2 c} =& \frac{1}{\sigma^2} \sum_{n=0}^{M-1} -A^2 \left(\frac{\partial r}{\partial c}\right)^2, \\ &+ (x[n] - Au[n])A \frac{\partial^2 u[n]}{\partial^2 c} \end{aligned} \tag{B.6}$$

$$\begin{aligned} \frac{\partial^2 \ln p}{\partial A \partial c} =& \frac{1}{\sigma^2} \sum_{n=0}^{M-1} -A \left(\frac{\partial u[n]}{\partial c}\right) u[n], \\ &+ (x[n] - Au[n]) \frac{\partial u[n]}{\partial c} \end{aligned} \tag{B.7}$$

$$\frac{du[n]}{dc} = -2\pi \sum_{l=0}^{L-1} h_l[n]\xi[n-l]\sqrt{\nu[n-l]}\sin(2\pi c\xi[n-l]). \tag{B.8}$$

Thus, the elements of the Fisher information matrix are

$$[I(\psi)]_{11} = -\mathrm{E}\left[\frac{\partial^2 \ln p}{\partial^2 A}\right] = \frac{1}{\sigma^2} \sum_{n=0}^{M-1} u^2[n],$$

$$[I(\psi)]_{12} = -\mathrm{E}\left[\frac{\partial^2 \ln p}{\partial A \partial c}\right] = \frac{1}{\sigma^2} \sum_{n=0}^{M-1} \left(Au[n] \frac{\partial u[n]}{\partial c}\right),$$

$$[I(\psi)]_{21} = [I(\psi)]_{12},$$

$$\begin{aligned} [I(\psi)]_{22} &= -\mathrm{E}\left[\frac{\partial^2 \ln p}{\partial^2 c}\right], \\ &= \frac{1}{\sigma^2} \sum_{n=0}^{M-1} \left(A \frac{\partial u[n]}{\partial c}\right)^2. \end{aligned}$$

ACKNOWLEDGEMENTS

This work was funded by the National Science Foundation under the contract NSF-ECCS 1102357 and by the Office of Naval Research MURI, Grant N00014-07-1-0739.

REFERENCES

1. Stojanovic M, Preisig J. Underwater acoustic communication channels: propagation models and statistical characterization. *IEEE Communications Magazine* 2009; **47**(1): 84–89.
2. Stojanovic M, Catipovic JA, Proakis JG. Phase-coherent digital communications for underwater acoustic channels. *IEEE Journal of Oceanic Engineering* 1994; **19**(1): 100–111.
3. Li B, Zhou S, Stojanovic M, Freitag L, Willett P. Multicarrier communication over underwater acoustic channels with nonuniform Doppler shifts. *IEEE Journal of Oceanic Engineering* 2008; **33**(2): 198–209.
4. Tu K, Fertonani D, Duman TM, Stojanovic M, Proakis JG, Hursky P. Mitigation of intercarrier interference for OFDM over time-varying underwater acoustic channels. *IEEE Journal of Oceanic Engineering* 2011; **36**(2): 156–171.
5. Tu K, Duman TM, Stojanovic M, Proakis JG. Multiple-resampling receiver design for OFDM over Doppler-distorted underwater acoustic channels. *IEEE Journal of Oceanic Engineering* 2013; **38**: 333–346.
6. Roy S, Duman TM, McDonald VK, Proakis JG. High-rate communication for underwater acoustic channels using multiple transmitters and space-time coding: receiver structures and experimental results. *IEEE Journal of Oceanic Engineering* 2007; **32**(3): 663–688.
7. Roy S, Duman TM, McDonald VK. Error rate improvement in underwater MIMO communications using sparse partial response equalization. *IEEE Journal of Oceanic Engineering* 2009; **34**(2): 181–201.
8. Stojanovic M. MIMO OFDM over underwater acoustic channels. In *Conference Record of the Forty-Third Asilomar Conference on Signals, Systems and Computers*, Monticello, IL, 2009; 605–609.

9. Emre Y, Kandasamy V, Duman TM, Hursky P, Roy S. Multi-input multi-output OFDM for shallow-water UWA communications (invited paper). In *Proceedings of ACOUSTICS 2008*, Paris, France, 2008; 5333–5338.
10. Kuperman WA, Hodgkiss WS, Song HC, Akal T, Ferla C, Jackson DR. Phase conjugation in the ocean: experimental demonstration of an acoustic time-reversal mirror. *The Journal of the Acoustical Society of America* 1997; **103**: 25–40.
11. Edelmann GF, Song HC, Kim S, Hodgkiss WS, Kuperman WA, Akal T. Underwater acoustic communications using time reversal. *IEEE Journal of Oceanic Engineering* 2005; **30**(4): 852–864.
12. Flynn JA, Ritcey JA, Rouseff D, Fox WLJ. Multichannel equalization by decision-directed passive phase conjugation: experimental results. *IEEE Journal of Oceanic Engineering* 2004; **29**(3): 824–836.
13. Song HC. Time reversal communication in a time-varying sparse channel. *The Journal of the Acoustical Society of America* 2011; **130**(4): EL161–EL166.
14. Yang TC, Yang W. Low probability of detection underwater acoustic communications using direct-sequence spread spectrum. *The Journal of the Acoustical Society of America* 2008; **124**(6): 3632–3647.
15. Ling J, He H, Li J, Roberts W, Stoica P. Covert underwater acoustic communications. *The Journal of the Acoustical Society of America* 2010; **128** (5): 2898–2909.
16. Severson J. Modeling and frequency tracking of marine mammal whistle calls. *Master's Thesis*, Massachusetts Institute of Technology, 2009.
17. Liu S, Qiao G, Ismail A. Covert underwater acoustic communication using dolphin sounds. *The Journal of the Acoustical Society of America* 2013; **133** (4): EL300–EL306.
18. Liu S, Qiao G, Ismail A, Liu B, Zhang L. Covert underwater acoustic communication using whale noise masking on DSSS signal. In *IEEE Oceans*, San Diego, CA, 2013; 1–6.
19. ElMoslimany A, Zhou M, Duman TM, Papandreou-Suppappola A. A new signaling scheme for underwater acoustic communications. In *IEEE Oceans*, San Diego, CA, 2013; 1–5.
20. Au WW. *The Sonar of Dolphins*. Springer-Verlag New York Inc.: New York, NY, 1993. P. 277.
21. Reynolds JE, III, Rommel SA (eds.) *Biology of Marine Mammals*. Smithsonian Institution Press: Washington, DC, 1999.
22. Tyack PL. Functional aspects of cetacean communication. In *Cetacean Societies: Field Studies of Dolphins and Whales*, Mann JR, Conner C, Tyack PL, Whitehead H (eds). The University of Chicago Press: Chicago, IL, 2000; 270–307.
23. Josso NF, Zhang JJ, Papandreou-Suppappola A, Ioanna C, Duman TM. Nonstationary system analysis methods for underwater communications. *EURASIP Journal on Advances in Signal Processing* 2011; **11**: 14.
24. Papandreou-Suppappola A. Biological signal analysis, detection, and estimation. *Technical Report 11284*, Naval Undersea Warfare Center, Newport, RI, December 2001.
25. Papandreou-Suppappola A, Suppappola SB. Sonar echo ranging using signals with non-linear time-frequency characteristics. *IEEE Signal Processing Letters* 2004; **11**: 393–396.
26. Papandreou-Suppappola A, Suppappola SB. Analysis and classification of time-varying signals with multiple time-frequency structures. *IEEE Signal Processing Letters* 2002; **9**: 92–95.
27. Watkins WA, Fristrup K, Daher MA, Howald T. SOUND database of marine animal vocalizations structure and operations. *Technical Report WHOI-92-31*, Woods Hole Oceanographic Institute, Woods Hole, MA, August 1992.
28. Kay SM. *Fundamentals of Statistical Signal Processing: Estimation Theory* (1st edn.), Prentice-Hall signal processing series, Vol. 1. Prentice-Hall PTR: Upper-Saddle River, NJ, 1993. P. 625.
29. Poor HV. *An Introduction to Signal Detection and Estimation* (2nd edn.) Springer-Verlag: New York, NY, 1988. Pp. 182–183.
30. Li W, Preisig JC. Estimation of rapidly time-varying sparse channels. *IEEE Journal of Oceanic Engineering* 2007; **32**(4): 927–939.
31. Berger CR, Zhou S, Preisig JC, Willett P. Sparse channel estimation for multicarrier underwater acoustic communication: from subspace methods to compressed sensing. *IEEE Transactions on Signal Processing* 2010; **58**(3): 1708–1721.
32. Wright SJ, Nowak RD, Figueiredo MAT. Sparse reconstruction by separable approximation. *IEEE Transactions on Signal Processing* 2009; **57**(7): 2479–2493.
33. Hodgkiss WS, Song HC, Dean G, Badiey M, Song A. Kauai Acomms MURI 2011 (KAM11) experiment trip report. *Technical Report*, August 2011.

AUTHORS' BIOGRAPHIES

Ahmad A. ElMoslimany received his BS degree from Ain Shams University, Cairo, Egypt, in 2009, MS degree from Nile University, Cairo, Egypt, in 2011, and PhD degree from Arizona State University, Tempe, Arizona, USA, in 2015, all in Electrical Engineering. Currently, he is working in Polaris Wireless, Mountain View, CA, USA. He was a Research Assistant in the Wireless Intelligent

Network Center (WINC) at Nile University from October 2009 to August 2011. From September 2011 to December 2015, he was a Graduate Research Associate at the Arizona State University. His research interest includes signal processing, information theory, channel coding theory, communications theory, wireless channel modeling, MIMO communications, and channel estimation.

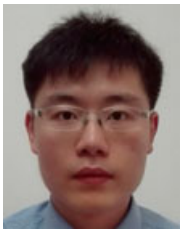

Meng Zhou received his BS degree in 2009 in Electronics and Information Engineering from the Huazhong University of Science and Technology (HUST), Wuhan, China. He received his MS degree in 2011 and PhD degree in 2014 from Arizona State University (ASU), Tempe, both in Electrical Engineering. He is currently working at Huawei Technologies Co., Ltd. His general research interests lie in the areas of signal processing and communication, including multiple target tracking and underwater acoustic communications. His recent focus is on optical fiber communications.

Tolga M. Duman is a Professor in the Electrical and Electronics Engineering Department of Bilkent University in Turkey and an Adjunct Professor in the School of ECEE at Arizona State University. He received his BS degree from Bilkent University in Turkey in 1993 and MS and PhD degrees from Northeastern University, Boston, in 1995 and 1998, respectively, all in Electrical Engineering.
Prior to joining Bilkent University in September 2012, he has been with the Electrical Engineering Department of Arizona State University first as an Assistant Professor (1998–2004), as an Associate Professor (2004–2008), and as a Professor (2008–2015). Dr. Duman's current research interests are in systems, with particular focus on communication and signal processing, including wireless and mobile communications, coding/modulation, coding for wireless communications, data storage systems, and underwater acoustic communications.
Dr. Duman is a Fellow of IEEE and a recipient of the National Science Foundation CAREER award and IEEE Third Millennium medal. He served as an Editor for IEEE Trans. on Wireless Communications (2003–2008), IEEE Trans. on Communications (2007–2012), and IEEE Online Journal of Surveys and Tutorials (2002–2007). He is currently the coding and communication theory area editor for IEEE Trans. on Communications (2011–present) and an editor for Elsevier Physical Communications Journal (2010–present).

Antonia Papandreou-Suppappola is a Professor of Electrical Engineering at the School of Electrical, Computer and Energy Engineering at Arizona State University, Tempe. She received her PhD degree in Electrical Engineering from the University of Rhode Island in 1995. Her research interests are in the areas of time-varying signal and system processing, and signal processing in wireless communications.
Dr. Papandreou-Suppappola received the IEEE Fellow award, NSF CAREER award, 2014 Fulton Exemplar Faculty award, 2013 Fulton School of Engineering award, 2010 Bob Owens Memorial Best Paper award in IEEE Workshop on Signal Processing Systems. She has served as Chair of Women in Signal Processing committee, IEEE Signal Processing Society (SPS) (2014–2017); Member-at-Large of IEEE SPS Board of Governors (2010–2012); Technical Committee Member of IEEE SPS on Signal Processing Theory and Methods (2003–2008); Treasurer of IEEE SPS Conference Board (2004–2006); and Associate Editor of IEEE Transactions on Signal Processing (2005–2009).